

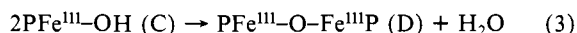
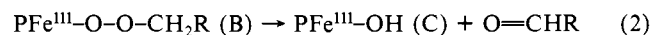
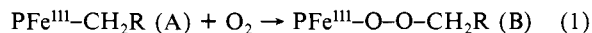
spectrum of C at $-70\text{ }^{\circ}\text{C}$ at the top and the sample after warming to $25\text{ }^{\circ}\text{C}$ and then recooling to $-70\text{ }^{\circ}\text{C}$. Most of C has decomposed to form the ultimate product, $\text{TTPFe}^{\text{III}}\text{-O-Fe}^{\text{III}}\text{TTP}$, D.⁶ Intermediate C has been prepared independently by treating a toluene- d_8 solution of $\text{TTPFe}^{\text{III}}\text{Cl}$ with sodium hydroxide,^{5,7} and this material converts to D under the conditions of Figure 2. Thus C is identified as the hydroxy complex $\text{TTPFe}^{\text{III}}\text{OH}$, which is known to undergo dehydration to give the oxo-bridged product.^{5,7}

Examination of the 0–10-ppm region of the ^1H NMR spectrum at $-70\text{ }^{\circ}\text{C}$ after the formation of C (but before conversion to D) shows the growth of a resonance (F in Figure 1) at 8.6 ppm which is consistent with the formation of formaldehyde. No evidence for the formation of methanol (at 3.0 ppm) is present in the spectrum. More convincing evidence for conversion of the alkyl group into the corresponding aldehyde comes from observations on $\text{TTPFe}^{\text{III}}\text{C}_2\text{H}_5$. Intermediates analogous to B and C are detected after low-temperature addition of dioxygen. Resonances at 9.14 ppm, q ($J = 3\text{ Hz}$) and 1.40 ppm, d ($J = 3\text{ Hz}$) are indicative of the formation of acetaldehyde. Traces of ethanol 3.30 ppm, q ($J = 7\text{ Hz}$) and 0.93 ppm, t ($J = 7\text{ Hz}$) are present. The ratio of acetaldehyde/ethanol is 96/4. No other organic products are detected.

Related observations have been made with $\text{TMPFe}^{\text{III}}\text{CH}_3$ (TMP is the dianion of tetramesitylporphyrin). Addition of dioxygen to a toluene- d_8 solution of $\text{TMPFe}^{\text{III}}\text{CH}_3$ requires a higher temperature ($-50\text{ }^{\circ}\text{C}$) to produce an intermediate analogous to B (pyrrole, 108 ppm). On standing at $-50\text{ }^{\circ}\text{C}$ for 1 h, this intermediate is converted into $\text{TMPFe}^{\text{III}}\text{OH}$ (pyrrole, 104 ppm), an analogue of C which is stable.⁵ During this process there is no evidence for the buildup of detectable concentrations of the previously identified intermediates, $\text{TMPFe}^{\text{III}}\text{-O-O-Fe}^{\text{III}}\text{TMP}$, $\text{TMPFe}^{\text{IV}}\text{=O}$, or $(\text{TMP}^{\bullet})\text{Fe}^{\text{IV}}\text{=O}$.^{2,3}

Intermediate B is identified as the hydroperoxide anion complex, $\text{PFe}^{\text{III}}\text{-O-O-CH}_2\text{R}$. The alternative formulation as the alkoxide complex $\text{PFe}^{\text{III}}\text{-OCH}_2\text{R}$ is untenable, since such alkoxide complexes are stable throughout the temperature range of our experiments and do not convert into $\text{PFe}^{\text{III}}\text{-OH}$ and $\text{PFe}^{\text{III}}\text{-O-Fe}^{\text{III}}\text{P}$.⁹

Our observations indicate that the oxygenation process proceeds via the three steps given in eq 1, 2, and 3. There are limited



precedents for conversion of other metal alkyl complexes into metal hydroperoxide anion complexes (eq 1).⁸ If reaction 1 occurs via homolysis of the Fe–C bond, the PFe^{II} product never diffuses far enough to allow for the formation of $\text{PFe}^{\text{III}}\text{-O-O-Fe}^{\text{III}}\text{P}$, the known product of the $\text{PFe}^{\text{II}}/\text{O}_2$ reaction under the conditions of our experiments.² Again, while the intimate details of reaction 2 are not wholly apparent, homolysis of the O–O bond to form $\text{PFe}^{\text{IV}}\text{O}$ and OCH_2R is a likely possibility. However, OCH_2R , if formed, must be rapidly oxidized by $\text{PFe}^{\text{IV}}\text{O}$ since very little alcohol, which would result from the reaction of OCH_2R with toluene, is produced.

Acknowledgment. We thank the National Institutes of Health (GM 26226) for financial support.

(6) La Mar, G. N.; Eaton, G. R.; Holm, R. H.; Walker, F. A. *J. Am. Chem. Soc.* **1973**, *95*, 63.

(7) Fielding, L.; Eaton, G. R.; Eaton, S. S. *Inorg. Chem.* **1985**, *24*, 2309.

(8) Fontaine, C.; Duong, K. N. V.; Merienne, C.; Gaudemer, A.; Giannotti, C. *J. Organomet. Chem.* **1972**, *38*, 167. Perree-Fauvet, M.; Gaudemer, A.; Boucly, P.; Devynck, J. *J. Organomet. Chem.* **1976**, *120*, 439. Lubben, T. V.; Wolczanski, P. T. *J. Am. Chem. Soc.* **1985**, *107*, 701. Lubben, T. V.; Wolczanski, P. T. *J. Am. Chem. Soc.* **1987**, *107*, 424.

(9) Note Added in Proof: This has been verified by ^2H NMR experiments which show distinctly different CD_2CD_3 resonances for $\text{TTPFeOCD}_2\text{CD}_3$ and $\text{TTPFeOOC}_2\text{CD}_3$.

Synthesis and Structure of the Iron–Selenium Cubane Cluster $[(\eta^5\text{-C}_5\text{H}_5)_4\text{Fe}_4\text{Se}_4]^{3+}$: The Fourth Member of the $[(\eta^5\text{-C}_5\text{H}_5)_4\text{Fe}_4\text{Se}_4]^n$ Series ($n = 0$ to $4+$)

Hiroshi Ogino,* Hiromi Tobita, Kasumi Yanagisawa, Mamoru Shimoi, and Chizuko Kabuto

Department of Chemistry, Faculty of Science
Tohoku University, Sendai 980, Japan

Received May 15, 1987

Transition-metal–chalcogen cubane system is one of the important models of understanding the relationship between electron count and geometrical structure of metal clusters. In contrast to sulfur derivatives,^{1,2} selenium derivatives have attracted less attention. Cyclopentadienyl iron–selenium derivatives, $[\text{Cp}_4\text{Fe}_4\text{Se}_4]^n$ ($\text{Cp} = \eta^5\text{-C}_5\text{H}_5$), only a series of organometallic metal–selenium cubane clusters reported so far, show four electrochemically reversible redox waves indicating the existence of five oxidation states, although only three of them, $n = 0$, $1+$, and $2+$, have been isolated and structurally characterized.^{3,4}

We report the synthesis and crystallographic determination of the fourth member of this oxidation series, $[\text{Cp}_4\text{Fe}_4\text{Se}_4]^{3+}$, the first cubane cluster possessing 17 skeletal electrons, based on high yield synthesis of the neutral and dicationic species.

Roder obtained $[\text{Cp}_4\text{Fe}_4\text{Se}_4]$ (**1**) in poor yield (2.7%) from the reaction of $[\text{Cp}_2\text{Fe}_2(\text{CO})_4]$ with commercial selenium in refluxing toluene.³ We found that the reaction of $[\text{Cp}_2\text{Fe}_2(\text{CO})_4]$ with red selenium Se_8 ⁵ ($3/8$ molar equiv) in toluene at $60\text{--}70\text{ }^{\circ}\text{C}$ for 2 days leads to the formation of **1** in almost quantitative yield. Dark brown crystals of **1** were isolated in 90% yield after removal of solvent and recrystallization by Soxhlet extraction with CH_2Cl_2 . Alternatively, the reaction of $[\text{Cp}_2\text{Fe}_2(\text{CO})_2(\mu\text{-Se})_2]$ ⁶ with commercial selenium in refluxing toluene for 2 h afforded **1** in 80% yield.

A cyclic voltammogram of **1** in CH_2Cl_2 containing 0.1 M ($n\text{-C}_4\text{H}_9$)₄NBF₄ (TBAB) as a supporting electrolyte shows four redox waves as shown in Figure 1a. Complexity of the cathodic waves from +0.7 to +0.2 V versus SCE is possibly due to the adsorption of polycationic cubane clusters on the electrode. The five oxidation states of the $[\text{Cp}_4\text{Fe}_4\text{Se}_4]^n$ system have been reported to be $n = 1-$, 0 , $1+$, $2+$, and $3+$.³ However, this assignment should be corrected to $n = 0$, $1+$, $2+$, $3+$, and $4+$ since the polarogram of a CH_2Cl_2 solution of **1** (Figure 1b) shows three anodic waves corresponding to three-step one-electron oxidation and no cathodic wave is observed.⁷

On the basis of this redox behavior of **1**, the bulk electrolysis of **1** was carried out in acetonitrile with 0.1 M NH_4PF_6 as a supporting electrolyte at +0.60 V versus SCE. After the usual workup, a dication salt, $[\text{Cp}_4\text{Fe}_4\text{Se}_4](\text{PF}_6)_2$ (**2**),³ was obtained in 90% yield. The dication salt **2** shows well developed four reversible, one-electron waves in 0.1 M TBAB acetonitrile.

Further oxidation to trication was achieved starting from **2**: Oxidation of **2** in acetonitrile in a manner similar to the synthesis of **2** at +1.0 V versus SCE followed by recrystallization from acetone gave $[\text{Cp}_4\text{Fe}_4\text{Se}_4](\text{PF}_6)_3\cdot\text{CH}_3\text{COCH}_3$ (**3**) as dark brown needles in 83% yield.⁸

The structure of the $\text{Cp}_4\text{Fe}_4\text{Se}_4$ unit in trication salt $[\text{Cp}_4\text{Fe}_4\text{Se}_4](\text{PF}_6)_3\cdot\text{CH}_3\text{CN}$ (**4**) is shown in Figure 2.⁹ Although

(1) Williams, P. D.; Curtis, M. D. *Inorg. Chem.* **1986**, *25*, 4562 and references therein.

(2) (a) Ferguson, J. A.; Meyer, T. J. *J. Chem. Soc., Chem. Commun.* **1971**, 623. (b) Trinh-Toan; Teo, B. K.; Ferguson, J. A.; Meyer, T. J.; Dahl, L. F. *J. Am. Chem. Soc.* **1977**, *99*, 408.

(3) Roder, R. M. Ph.D. Thesis, University of Wisconsin—Madison, Madison, WI, 1973.

(4) Szmanda, C. R. Ph.D. Thesis, University of Wisconsin—Madison, Madison, WI, 1979.

(5) Bagnall, K. W. *The Chemistry of Selenium, Tellurium and Polonium*; Elsevier: Amsterdam, 1966.

(6) Haines, R. J.; Debeer, J. A.; Greatrex, R. *J. Organomet. Chem.* **1975**, *85*, 89.

(7) We have recently found that the sulfur analogue, $[\text{Cp}_4\text{Fe}_4\text{S}_4]^n$ also takes five oxidation states assigned to $n = 0$, $1+$, $2+$, $3+$, and $4+$, instead of $n = 1-$, 0 , $1+$, $2+$, and $3+$ as reported previously.²

(8) Anal. Calcd for $\text{C}_{23}\text{H}_{26}\text{F}_{18}\text{Fe}_4\text{O}_3\text{P}_3\text{Se}_4$: C, 21.37; H, 2.03. Found: C, 21.37; H, 2.23.

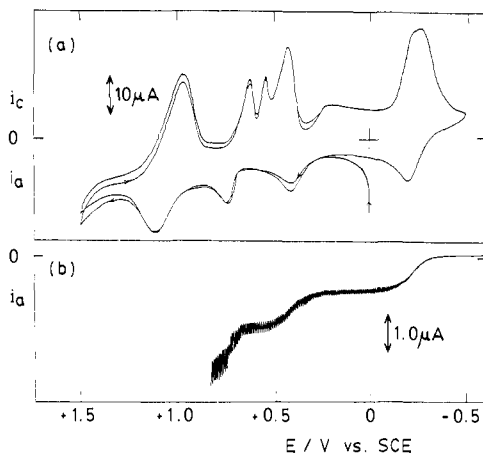


Figure 1. (a) Cyclic voltammogram of $[\text{Cp}_4\text{Fe}_4\text{Se}_4]$ (**1**) in 0.1 M TBAB CH_2Cl_2 by a platinum electrode: scan rate 50 mV s^{-1} , $[\mathbf{1}] = 2.5 \times 10^{-4} \text{ M}$. (b) DC polarogram of **1** in 0.1 M TBAB CH_2Cl_2 , $[\mathbf{1}] = 2.5 \times 10^{-4} \text{ M}$.

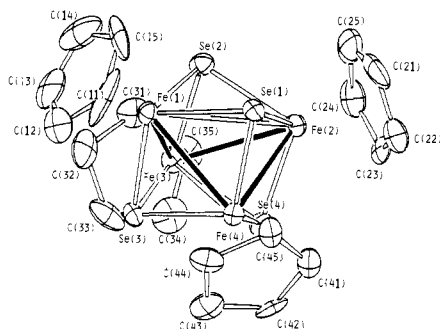


Figure 2. Perspective view of one of the two crystallographically independent tetracations in $[\text{Cp}_4\text{Fe}_4\text{Se}_4](\text{PF}_6)_3 \cdot \text{CH}_3\text{CN}$. Selected interatomic distances: Fe(1)–Fe(2), 3.358 (4) Å; Fe(3)–Fe(4), 3.353 (3) Å; Fe(1)–Fe(3), 2.839 (3) Å; Fe(2)–Fe(4), 2.802 (4) Å; Fe(2)–Fe(3), 2.933 (4) Å; Fe(1)–Fe(4), 2.777 (3) Å.

there are two kinds of crystallographically independent cationic clusters, their structures are almost the same, with some differences in the orientations of cyclopentadienyl rings. The cubane cluster can be described as a tetracapped tetrahedron with a pseudo- S_4 axis. The four Fe–Se bonds parallel to the axis are shorter (2.260 (3) ~ 2.270 (3) Å) than the others (2.311 (3) ~ 2.350 (3) Å). Four of the six Fe–Fe distances (2.760 (4) ~ 2.974 (4) Å) are shorter than the others (3.353 (3) ~ 3.358 (4) Å) which are perpendicular to the pseudo- S_4 axis. The Fe_4 core of $[\text{Cp}_4\text{Fe}_4\text{Se}_4]^n$ shrinks uniformly with the increase of the charge of the cubane cluster: The average Fe–Fe distances are 3.28, 3.20, 3.11, and 3.02 Å, for the clusters of $n = 0$,³ $1+$,⁴ $2+$,³ and $3+$, respectively. This tendency is due to the stepwise removal of antibonding electrons from the neutral cluster.⁴

$[\text{Cp}_4\text{Fe}_4\text{Se}_4]^n$ is the first example of a cubane cluster on which the species of four successive oxidation states are isolated and crystallographically characterized.

Acknowledgment. The present study was supported by a Grant-in-Aid for Scientific Research, no. 60430011, from the Ministry of Education, Science and Culture.

Supplementary Material Available: X-ray crystallographic data for **4** (13 pages). Ordering information is given on any current masthead page.

(9) **4** was crystallized from acetonitrile–dichloromethane. Crystal data as follows: $\text{C}_{22}\text{H}_{23}\text{F}_{18}\text{Fe}_4\text{NP}_6\text{Se}_4$, FW = 1275.6, monoclinic, space group $P2_1/a$, $a = 20.798$ (4) Å, $b = 17.580$ (3) Å, $c = 19.743$ (3) Å, $\beta = 106.41$ (1)°, $V = 6924.5$ (21) Å³, $Z = 8$; $D_c = 2.45 \text{ g cm}^{-3}$; $\mu(\text{Mo K}\alpha) = 6.47 \text{ mm}^{-1}$. Intensities of 8950 reflections were measured at 13 °C ($2^\circ < 2\theta < 52^\circ$) on a Rigaku AFC-5R diffractometer by using graphite monochromated Mo K α (0.71073 Å) radiation. The structure was solved by the direct method (MULTAN). For 5849 unique reflections ($|F_o| > 3\sigma(F_o)$) the atomic parameters were refined to $R = 0.068$ ($R_w = 0.087$). Details will be reported elsewhere.

Nitrile Hydratase: The First Non-Heme Iron Enzyme with a Typical Low-Spin Fe(III)-Active Center

Yukio Sugiura* and June Kuwahara

Faculty of Pharmaceutical Sciences
Kyoto University, Sakyo-ku, Kyoto 606, Japan

Toru Nagasawa and Hideaki Yamada

Department of Agricultural Chemistry
Kyoto University, Sakyo-ku, Kyoto 606, Japan

Received March 10, 1987

Nitrile hydratase isolated from *Brevibacterium* R312¹ and *Pseudomonas chlororaphis* B23² is a new iron-containing enzyme which catalyzes the hydration of aliphatic nitriles to the corresponding amides: $\text{RCN} + \text{H}_2\text{O} \rightarrow \text{RCONH}_2$. This enzyme is clearly distinguishable from nitrilase that directly converts nitrile to the corresponding acid and ammonia: $\text{RCN} + 2\text{H}_2\text{O} \rightarrow \text{RCOOH} + \text{NH}_3$. The efficient enzymatic transformation of nitrile into amide is useful for bioindustry. No information on the iron center of nitrile hydratase is obtained; however, it is known that no heme iron and no acid-labile sulfur are contained in nitrile hydratase.^{1,2} Herein, we decided to apply electron spin resonance (ESR) spectroscopy to characterize the iron state of the enzyme and found that nitrile hydratase is the first non-heme iron enzyme containing a typical low-spin Fe(III)-active site.

Nitrile hydratase was purified from the crude extract of *Brevibacterium* R312 ($M_w = 85\,000$ and subunit = 3) or *Pseudomonas chlororaphis* B23 ($M_w = 100\,000$ and subunit = 4) according to our previous reports.^{1,2} The crystallized enzymes were homogeneous by polyacrylamide gel electrophoretic and ultracentrifugal analyses. In the enzyme samples, no significant concentrations of transition-metal ions, other than iron, were detected by X-ray fluorescent analysis. Even the dialysis for 48 h at pH 7.5 or pH 6.5 showed no liberations of iron from the enzymes, indicating that the iron atoms are tightly bound to the protein. H_2^{17}O (31.0 atom %) was purchased from B.O.C. Limited, United Kingdom. ESR measurements were run on a JES-FE-3X spectrometer equipped with a liquid nitrogen Dewar flask as a sample holder. The ESR spectra were quantitated by double integration versus a 1 mM copper(II) EDTA standard, with use of the g value corrections of Aasa and Vänngard.³

Figure 1A shows ESR spectrum of native nitrile hydratase isolated from *Brevibacterium* R312 at 77 K. Double integration of the spectrum gave 2.9 ± 0.2 spin per enzyme molecule. The result is consistent with the estimation (2.9 ± 0.1 atoms iron/mol enzyme) of iron analysis by an atomic absorption method, indicating that the enzyme contains one atom iron per subunit. Treatment of a reducing agent such as dithiothreitol to nitrile hydratase resulted in no significant changes of the ESR signals. Of special interest is the fact that the ESR features ($g_{\text{max}} = 2.284$, $g_{\text{mid}} = 2.140$, and $g_{\text{min}} = 1.971$) of the present enzyme are characteristic of rhombic low-spin Fe(III) ($S = 1/2$) type. The iron enzyme is a non-heme iron enzyme but not hemoprotein and ferredoxin because of no existence of iron–porphyrin and acid-labile sulfur.^{1,2} Indeed, the estimated g values differ distinctly from those ($g = 2.05$, 1.94, and 1.88) of a typical iron–sulfur cluster.⁴ In reduced ferredoxin or aconitase, an ESR signal at $g = 1.94$ or 2.01 is attributed to a spin-coupled binuclear or trinuclear iron–sulfur unit.⁵ In an enzymatically active reduced form of purple acid phosphatase, a novel ESR signal centered at

(1) Nagasawa, T.; Ryuno, K.; Yamada, H. *Biochem. Biophys. Res. Commun.* **1986**, *139*, 1305–1312.

(2) Nagasawa, T.; Nanba, H.; Ryuno, K.; Takeuchi, K.; Yamada, H. *Eur. J. Biochem.* **1987**, *162*, 691–698.

(3) Aasa, R.; Vänngard, T. *J. Magn. Reson.* **1975**, *19*, 308–315.

(4) Beinert, H. In *Iron–Sulfur Proteins III*; Lovenberg, W., Ed.; Academic Press: New York, 1977; pp 61–100.

(5) Kent, T. A.; Dreyer, J.-L.; Kennedy, M. C.; Huynh, B. H.; Emptage, M. H.; Beinert, H.; Münck, E. *Proc. Natl. Acad. Sci. U.S.A.* **1982**, *79*, 1096–1100.